RSC Advances

PAPER

View Article Online
View Journal | View Issue

Cite this: *RSC Adv.*, 2022, **12**, 2888

Macro and micro thermal investigation of nanoarchitectonics-based coatings on cotton fabric using new quaternized starch

Zeeshan Ur Rehman,[a] Mosab Kaseem,[b] David G. Churchill,*[c] Ye-Tang Pan[d] and Bon Heun Koo*[a]

Implementation of a new cationizing reagent and its incorporation onto the backbone of starch was performed successfully, confirmed from the remarkable micro- and macro anti-flammable properties. The morphologies and localized compositional analysis of the modified starch-based LBL coatings on the cotton surface were carried out using LV-SEM and EDX: highly uniform coating layers and uptake of solution species for intermediate implant reagent concentrations were confirmed. The subject samples were further analyzed through thermogravimetric analysis (TGA), microcombustion experiments (MCC), flame testing (VFT) and afterburn measurements. The peak range of the degradation was highly improved from the lower range to the higher range (329.92–394.48 °C), together with significant mass residue for TBAB-0.7–17.02%. Moreover, a significant decrease in the absolute heat loss (THR ∼ 30%), heat dissipation competence (HRC ∼ 27.86%), and peak heat output (PHRR ∼ 23%) was achieved for a TBAB loading of ∼0.7 g. The results were further confirmed from the increase in the limiting oxygen index (LOI) to a higher rate of ∼23.2, improved structural integrity and higher quality of char obtained in the VFT and after-burn analysis.

Received 20th December 2021
Accepted 7th January 2022

DOI: 10.1039/d1ra09197b

rsc.li/rsc-advances

1. Introduction

Use of bio-molecules in fire retardants is a persistent and immediate demand to cope with the fire vulnerability of products together with the fire hazards of the existing synthetic materials. One of the most fire vulnerable, albeit domestic and increasingly being considered in the high tech, is cotton fabric. Cotton fabric is known to people of all civilizations, and being used in enormous quantities due to no other better alternatives, due to its abundance and relationship to humans and environmentally friendly aspects. However, its current use and future boosted applications are threatened by its limited chemistry which is in favor of lower flammability ratings such as limiting oxygen index (LOI) ∼19.0, and lower combustion temperature (360–425 °C).[1] The fire vulnerability of these products could cause serious fire accidents and fatalities in industrial buildings and domestic residences.[2] However, the chemistry of cotton as it comes to us from nature is largely unchangeable; extrinsic strategies therefore are applied to cope with these issues, *e.g.*, surface grafting techniques,[3] ultraviolet curing of polymers,[4] flame retardant finishing treatments,[5] sol–gel methods of thin-film deposition,[6] plasma treatments,[7] and layer-by-layer (LBL) coating techniques.[8–12]

These methods offered successful results, however the major objective towards the commercialization was hindered by a few major flaws such as the use of synthetic materials, cost issues, operational complexities, and a shift in the mechanical properties of the cotton substrate. Comparatively, the LBL method, although having newly entered into the fire-retardant field, offered excellent figures of merit. LBL methodology in general has been developed and studied extensively by multiple research groups in the past two decades.[13,14] According to this method, nano-architecting of thin films can be carried out on a substrate by the process of dipping or spraying the subjected material alternatively into suspensions/solutions of polymers or particles-based polyelectrolyte dilute aqueous solutions/mixtures (<1 wt% solids).[15,16] Several weak and strong chemical interactions, such as electrostatic interactions, hydrogen bonding[17] donor/acceptor interactions,[18] and covalent connections[19] can play vital roles in the fabrication of these multilayered films. The potential and magnitude of such factors are substantially influenced by the formulation and delicate conditions pertaining to the chemistry of the layer components, counterions,[20] molecular weight,[21] ionic strength,[22] and the pH of the dipping solutions/mixtures, as well as the experimental

[a]*Nano and Advance Materials Engineering, Changwon National University, Changwon, Republic of Korea. E-mail: bhkoo@changwon.ac.kr*
[b]*Department of Nanotechnology and Advanced Materials Engineering, Sejong University, Seoul, 05006, Republic of Korea*
[c]*Department of Chemistry, Korea Advanced Institute of Science and Technology, Republic of Korea. E-mail: dchurchill@kaist.ac.kr*
[d]*National Research Center of Flame Retardant Materials, Beijing Institute of Technology, Beijing, PR China*

temperature,[23] which might serve to control coating thickness, which, typically ranges from 1–100 nm.

To help obtain fire retardant coatings based on the LBL process, green materials, acquired from either plants or animals, such as chitosan, lignin,[24] tannic acid,[25,26] deoxyribonucleic acid,[27] cellulose nanofibers, starch[28] and phytic acid became optimistic and practical potential fire retardant agent component choices toward textiles and discrete polymeric materials.[29] Among them, starch has one of the largest natural reserves: a mixture constituting two biomolecules, composed of anhydrous glucose units, amylose, and amylopectin. The use of starch (thermoplastic starch) for fire retardant research applications considering its bioavailability *etc.* was initiated by Kun Wu *et al.*, and it assisted to trigger FR composites with diverse chemical complexes. These composites achieved V-0 ratings.[30]

Coatings based on starch were first prepared by Tsuyumoto *et al.* through the use of starch and sodium polyborate (SPB) as an electrolyte; the material was enforced over persistent polyurethane (RPU) foam, polyethylene terephthalate (PET), as well polypropylene (PP). Throughout the burning test, it was found that the coated substrates (10 mm thickness) repelled the premixed flame (length = ~100 mm), for more than 12 min.[31] Davis *et al.* reported the use of a one-pot method to help produce flexible fire resistive thin films on polyurethane foam by using starch–boric acid–MMT clay matrixes; the authors obtained a 63% reduction in flammability values.[32] Carosio *et al.* for the first time prepared LBL-based coatings on cotton, using starch merged with poly(phosphoric acid). With the 30% gain in the residue mass constituted an improvement; however, the authors used additional synthetic polyelectrolytes and obtained a very low degradation temperature ~290 °C.[28] Mallick *et al.* employed a system of grafted starch and mica to form nanocomposite hydrogels through emulsion polymerization techniques and obtained delayed ignition times and peak heat release rates.[33] Subsequently, Choi *et al.* investigated a new polyelectrolyte system, comprised of starch–clay (MMT; montmorillonite) on cotton fibers and acquired improved afterglow time and char debris from the VFT analysis.[34] More recently, Owodunni *et al.* reported the use of starch as a binder to manufacture particleboard from coconut fibers and obtained enhanced fire-retardant properties.[35] However, despite all these efforts, scientists studying such starch-based materials are still anticipating the full emergence of these materials as fire-retardant ingredients due to intrinsic deficiencies such as facile hydrolysis and the material's neutral (nonionic) nature.

To solve the issue of the non-ionic nature of starch, chemical (post) modification is a well-known pre-requisite to impart charge to the (macro) molecular structure and thus validate its use for multiple applications. Chemical modification is generally carried out by frequently treating of starch-based materials with modifying agents. Such chemicals are designed to undergo reactions with hydroxyl groups; they may be able to be grafted with other common polymers. Cationization means the attainment of a positively charged nature; this is a simple and known protocol whereby starch derivatives can retain a plus charged (+) atoms or group of atoms (such as $=^{+}NH-$, $^{+}NH_4$ *etc.*) within their monomeric units through a wide spectrum of pH values. Furthermore, the induction of a cationic group can impart a significant mineral binding properties to the building block of a starch. The cationized starch can be used further with an appropriate polyanionic material such as clays, nanostructures, and organic components to form LBL coatings.

Vermiculite ($(MgFe,Al)_3(Al,Si)_4O_{10}(OH)_2\cdot 4H_2O$) and montmorillonite clay-based materials ($(Na,Ca)0.33(Al,Mg)_2(Si_4O_{10})(OH)_2\cdot nH_2O$, MMT) are common and relatively inexpensive materials that can be considered as ingredients for such flame retardant composites. These are of vital interest to assist forming fire retardant matrixes over starch, based on the LBL method. Vermiculite clay (VMT) has remarkable flame retarding features.[36] For example, when VMT is exposed to excessive thermal energy (>200 °C), its chemical structure undergoes exfoliation. In particular, the material releases water molecules from within its structure, molecules located within interlayer sheets.[37] Such structural exfoliation phenomena of materials such as VMT which inhibit thermal transfer and molecular migration when exposed to heat, allows these materials to demonstrate significant flame retardant properties and be classified as self-intumescent materials.[37,38] Very recent research reports have proposed the effectual model of VMT and MMT clay for LBL-based fire-retardant coatings.[39–43] As a consequence, herein, a miscellaneous network of VMT/MMT clay (1/1%) in (aqueous solution) has been utilized as an anionic source and starch (cationized form) the corresponding counter-ion species to help produce a new flame-retardant nanocomposite thin layer material on cotton tissue. Moreover, starch was chemically cationized (*vide supra*) using various concentrations of a quaternary ammonium salt and then used for LBL coatings. The effect of various concentrations on the cationization agent on the properties of coatings and the fire-retardant characteristics were investigated.

2. Materials and substrates

All materials were used as obtained from commercial sources unless otherwise mentioned. Montmorillonite (MMT, 99%) was obtained from Sigma Aldrich. Vermiculite (VMT) clay and cotton fabric were obtained from local company. Deionized water with conductivity ~1.4 μS cm^{-1} was prepared freshly. Polyacrylic solution (25%) was obtained from Fujifilm Wako and was further hydrated till reach 1.2%, in order to maintain pH of 1.8. For cationization process the chemicals used were as TBAB (≥98.0%), NaOH (reagent grade, ≥98%), Na_2SO_4 (≥99%) were respectively obtained from Sigma Aldrich.

To help obtain the LBL coatings, an anionic suspension (1%) was prepared by mixing an equal amount of montmorillonite (MMT) and vermiculite (VMT) clay into deionized water. Differently from the anionic solution, 2% suspension of the cationized starch was used in the cationic solution. The suspension was homogenized through an extended period of stirring lasting about 48 h. A semi-transparent hydrogel was finally obtained after the stirring process. Cotton fabric (100%, 180 g m^{-2}) was divided carefully into pieces (height/width ~ 230 mm/120 mm), cleaned, and dried before experimental use. For the LBL techniques, the desiccated cotton was then pre-processed in the polyacrylic solution (1.2%, pH; 1.8) for the next 20 min.

3. Experimental

3.1 Cationization process

The process of chemical cationization of the individual units of starch was carried out using well-known protocol reported previously.[44] However, a novel implanting agent was used and examined to perform the process of cationization. As mandated by the calculated values based on this procedure, 12.0 g of potato starch and 8 g of Na_2SO_4 were mixed in 25 mL of alkaline ethanol (1.7 g NaOH) to afford a slurry. This mixture was shaken while being heated for 10 min. Heating was performed simply in a water bath at a constant temperature of 50 °C. Afterwards, 2.0 g of tetrabutylammonium bromide (TBAB) was added to the solution to effect chemical cationization. The obtained mass was then subsequently blended vigorously and then incubated for next 6 h under the same temperature. Finally, an acidic alcoholic solution (3 N HCl in ethanol) was used to neutralize the whole stock, before being filtered, isolated and purified by washing through centrifugation and decanting of the supernatant liquid. The same process was repeated by varying the concentration of the implanting reagent (TBAB) from 0.5–2.0 g. The prepared cationized powder was then used for each LBL process.

3.2 Layer-by-layer assembly

The process of assembly involved a layer-by-layer approach which is a sequential experimental approach. Repeated deposition of films will naturally allow for one layer to be deposited upon the previous one. Importantly, the submerged cotton was first dipped into an electrolyte solution, the cationic solution; then, into MMT/VMT (anionic) suspension mixture agent solution. Finally, there was a rinsing step involving deionized water. After these three dipping steps are performed, one cycle is pronounced complete. Each time a new substrate was treated, the first step required submerged in each container for 5 min. The second step, however, required only 2 min per each dipping, each time followed by a rinsing and drying step of the substrate. Desired number of bilayers ~7, under each condition of TBAB concentration (0.5–2.0 g) were deposited on the substrate and were consequently named as; **TBAB-0.5**, **TBAB-0.7**, **TBAB-1.0**, **TBAB-2.0** respectively. Subsequently depositing required amount of bilayers, the samples were finally air dried at ~80 °C. The experimental protocol and resistance offering phenomenon of the LBL coatings can be explored as shown in Fig. 1.

3.3 Characterization and measurements

Using a low voltage scanning electronic microscope (LV-SEM, Merlin compact), the surface morphologies of the coated and the untreated fabric samples, as well as their char residues, were examined. EDX (energy-dispersive X-rays spectroscopy) was used as a combined means of characterization along with LV-SEM to help examine the elemental composition of the coating surfaces (*vide infra*). For the effective surface microscopy, the as-coated fabric samples were Pt-sputtered for short period of 3 min, subject to a high vacuum to help transmit

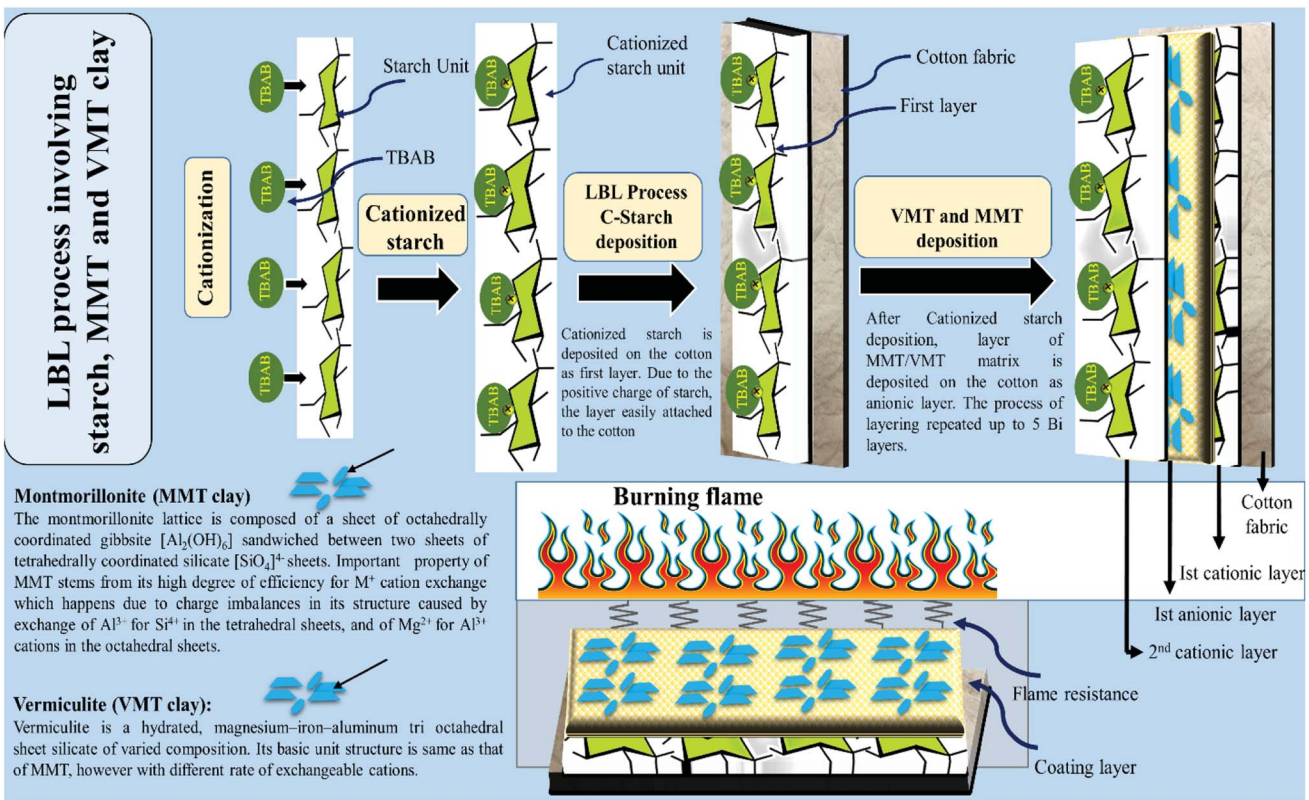

Fig. 1 Stepwise schematic diagram of starch cationization, LBL layering and resistance against flame.

conduction to the fabric surface. Microscale combustion analysis was conducted by using a FTT Microscale combustion calorimeter (MCC) in accordance with the ASTM D7309-13 suggested guidelines. Each sample, weighing approximately 10-15 mg were taken in platinum pans, (measured thrice) was heated at ~100 °C for at least 5 minutes, before being burned at 20 °C min^{-1} up to 600 °C, keeping the oxygen/nitrogen flow pace at 20/80 (mL). Macro-combustion tests such as vertical flame test (VFT) was performed for each coated and the control sample, in conformity with documented ASTM D6413 standards. Accordingly, the samples were combusted in a lab-made vertical flammability box (300 mm × 120 mm), using a Bunsen burner flame; the flame was applied for 10 seconds, exactly 20 mm below the fabric sample and the process was recorded using a high speed optical camera.

4. Result and discussion

4.1 Activation process and multilayers formation

The partial negative charge on oxygen atoms "O" and positive charge on the carbon-6 "C_6" in the unit cell of starch make this chemical group more vulnerable to nucleophilic attack by the quaternary ammonium bromide. As shown in Fig. 2, during the cationization process, the "C_6" atom of the starch, particularly that of the amylose linear chain, which is more easily accessible, is activated through OH^- ions origination from the added NaOH concentration. The activation of the "O" at "C_6" causes a further increase in the polarization intensity of the "π" bond between "C_6" and "O" atoms. At the moment, when the nucleophile energy is enough to break the "π" bond between "C_6" and "O", the attack of nucleophile occurred on "C_6" and it becomes attached to the starch on "C_6" position. The NaOH will deprotonate the OH and allow for the sodium alkoxide unit which is then covered to the ammonium alkoxide with elimination of NaBr as by product. It is important to mention that several parameters need be modified in order to achieve a higher degree of chemical substitution (DS) and therefore more complete cationization: (a) the quantity of NaOH should be sufficient to help trigger an effect on the exterior –OH groups in the starch macromolecule; nevertheless, increasing the concentration of NaOH could result in mercerization, which would result in the polymer structure adopting some level of crystallinity.[45] (b) The chemical reaction gape supposed to be enough as to increase the degree of substitution,[46] as well as starch degradation in the corresponding basic solution, (c) the elevated molar ratio values of TBAB toward AGU could allow for greater availability of regents and thus higher DS.[47] However, the maximum use of TBAB/starch AGU could pose further complications; thus optimized ratio should be used. (d) Finally, the uniformity of the process should be ensured, since the homogeneous dissemination of the elements provide for the improved availability of the OH groups, otherwise preferential cationization will result, along with the natural preferential distribution due to the easy accessibility of the linear amylose chain, compared to branched amylopectin. Scheutjens–Fleer theory[19] can be used to describe the mechanism of multilayer layer formations being that of an electrolyte substance add-on with the cotton tissue surface.[15] According to this theory, the most prominent factors are the surface charge density (σ0), charge on polymer (qm), and its ionic strength (cs) could influence the synergy of polyelectrolyte substances at the interface of the solid–liquid system. In addition, other non-ionic dynamics are supposed to have a substantial impact on the adsorption of polyelectrolyte such as the adsorption energy parameter "χs".[48] The process of cationization was used to acquire charge on the starch surface in the following cationic solution, whereas for an anionic electrolyte mixture of VMT/MMT were used. As a consequence of having opposite charges in the cationic and anionic solutions, the components of the solutions seem to be attach to the oppositely charged surface areas and thus could develop layers. Before performing the LBL process, the cotton substrates were kept in a 1% PAA solution for 20 min to help impart a negative charge surface.

4.2 Analysis of the microstructure and analysis of the materials

The resulting coated materials were imaged and the coating morphology can be explained from this imaging data. Morphologies of the fabrics which were coated – and also uncoated (control) – are provided in Fig. 3a–e. The surface of the uncoated samples has a highly smooth and polished topology (Fig. 3a). On the contrary, the surface of the coated fabric can be seen as covered by the layers uniformly, by the components of the electrolytes, which contribute to the observed rough and jagged topology. The fibers can be seen as being broken at multiple locations due to the soaking process as indicated by arrows in the graph. The sheet-like structures can also be observed on the surface and are believed to be the VMT species. The cross-sectional foliage of the alternate layers and the embedded VMT/MMT particles can also be observed from the single fiber images (Fig. 4a–e). It can be discerned that the coated specimens have a grid of layers on the surface, whereas the uncoated samples have a smooth and singular topology.

Furthermore, it is presumed that LBL layers could follow two modes of deposition: precipitate formation and uniform layer matrix formation. The precipitate mode of deposition could result from the mutual particle/polyelectrolytes and particle/particle interactions as reported elsewhere.[49] Such interactions form agglomerated species, which could randomly adhere to the cotton fibers. It can be further seen from the single fiber images that the coating layers are more evident in **TBAB-0.7** and **TBAB-1.0**, suggesting excellent adsorption of the solution species. In comparison, samples of **TBAB-0** and **TBAB-2.0** materials are relatively smooth due to the lower adsorption of solution species. The lower adsorption on the **TBAB-2.0** might have occurred due the macroscopic size of the starch polymer chains upon the attachment of a large quantity of quaternary molecules. The bulky layers suggest a higher intake of solution components (VMT/MMT); this could lead to excellent fire-retardant effects upon testing. It was noticed that for a small number of layers (7BL) as in this study, the cross-contamination has a minor effect on the exchange and adsorption process; thus, it has insignificant effects on the thickness of the final

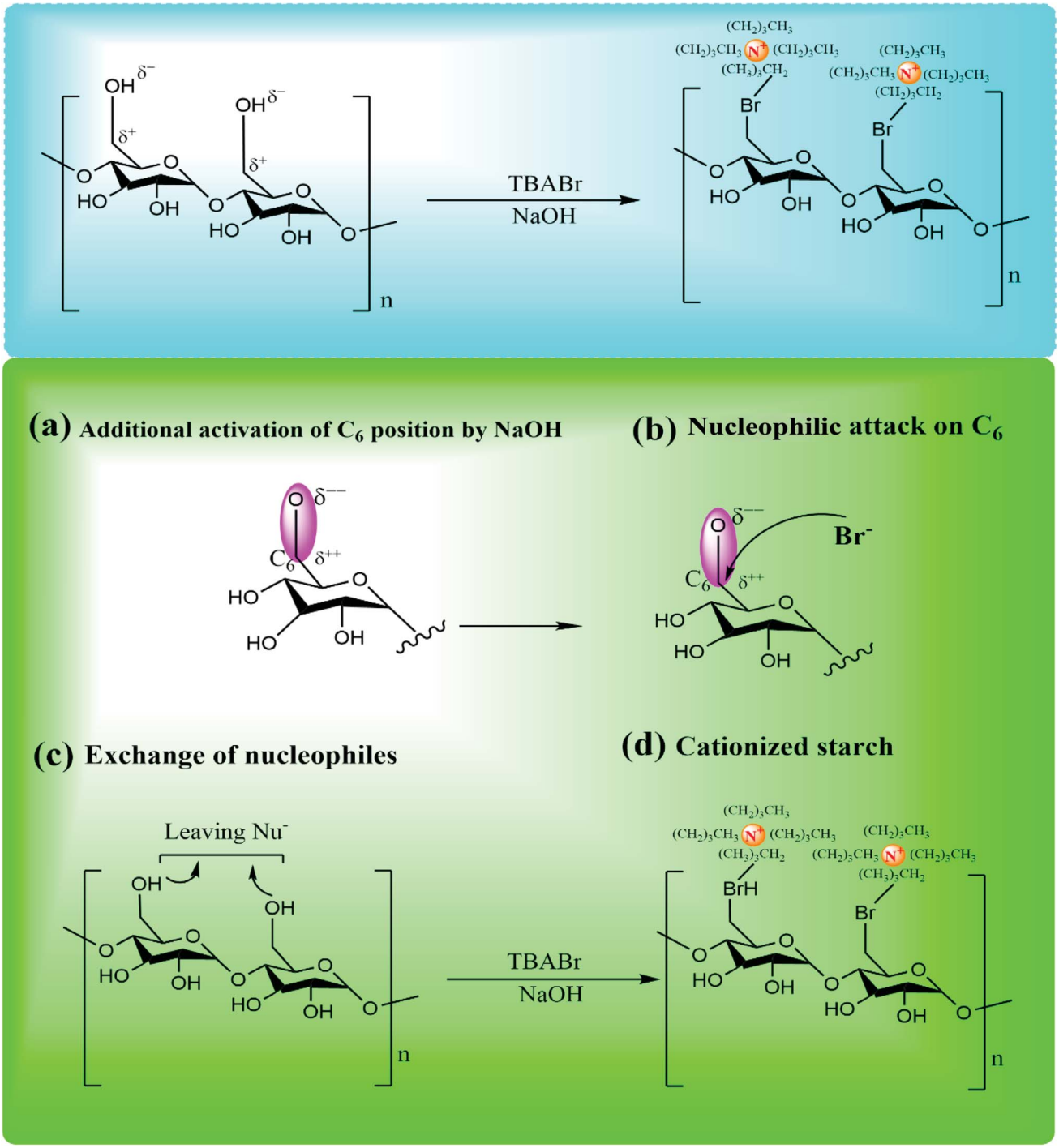

Fig. 2 Proposed reaction mechanism of the cationization of starch.

coatings. However, for an increased number of layers, the cross-contamination effect should be considered and so its effect on the thickness, due to the number of alterations of charge that were experienced by the material.

The EDX spectra of all the samples can be clearly observed in Fig. 5; the composition percentages are summarized in Table 1. The uncoated fabric could not show any peak of the solution components due to the absence of any coating layers. On the contrary, the intake of starch and clay species can be confirmed from peaks of the obtained component parts (C, O, Co, Na, Mg, Al, Si, K, S, Ca, *etc.*). One can gather, from the peak intensity of the clay species that the trend is increasing linearly with TBAB concentration. The highest intensities of the species (Al, Si… *etc.*) as encircled, can be obtained for **TBAB-0.7**. However, a further increase in the TBAB concentration did not cause any significant alteration in the intake of clay components

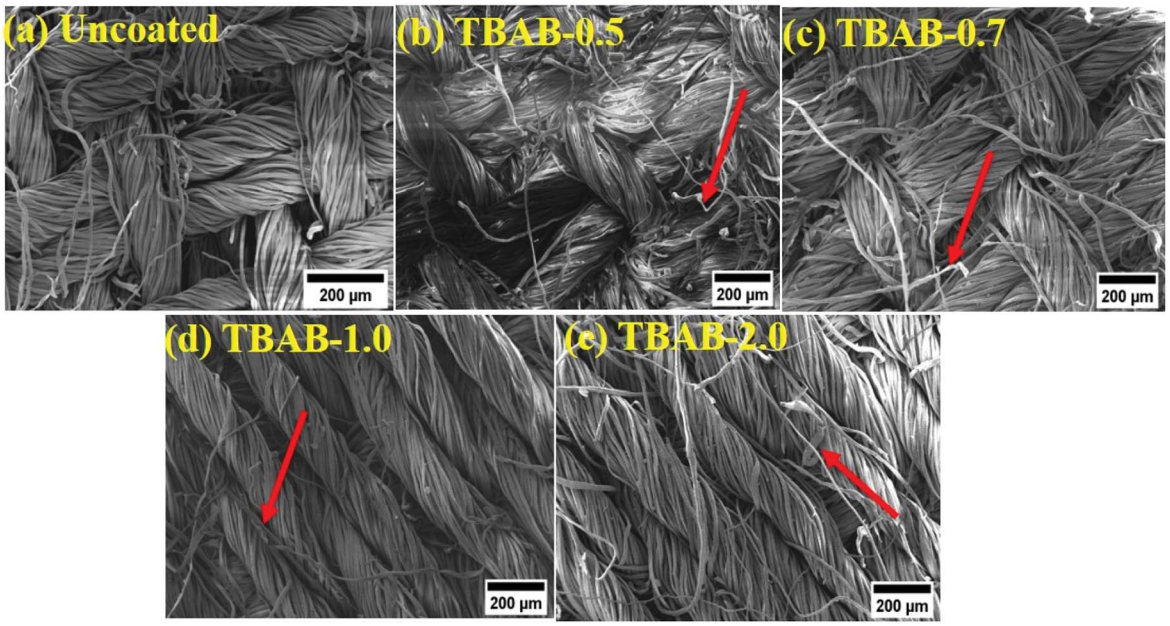

Fig. 3 (a–e) LV-SEM surface morphologies of the uncoated and coated fabric samples.

suggesting no further significant role in the cationization intensity of the starch. The presence of the clay component elements in the EDX profile can help researchers predict enhanced fire-retardant performance of the cotton fibers compared to the uncoated samples (control samples).

4.3 Thermal stability

To help analyze the thermal and thermo-oxidative stability, TGA and DTGA curves were drawn as shown in Fig. 6a and b; the summarized data are provided in Table 2. The TGA curves can be divided into three sections with respect to the weight loss; T_{onset}, major pyrolysis region and T_{offset}. It can be seen that the weight losses for the mid region and T_{offset} are highly aggressive compared to that value at T_{onset}. The highest value of $T_{onset} \sim 329.9\ ^{\circ}C$ and $T_{offset} \sim 394.5\ ^{\circ}C$ could be observed for **TBAB-0.7**; this which suggests excellent behavior against the burning process. The range of major degradation zones has been reported differently by various authors for starch-based LBL

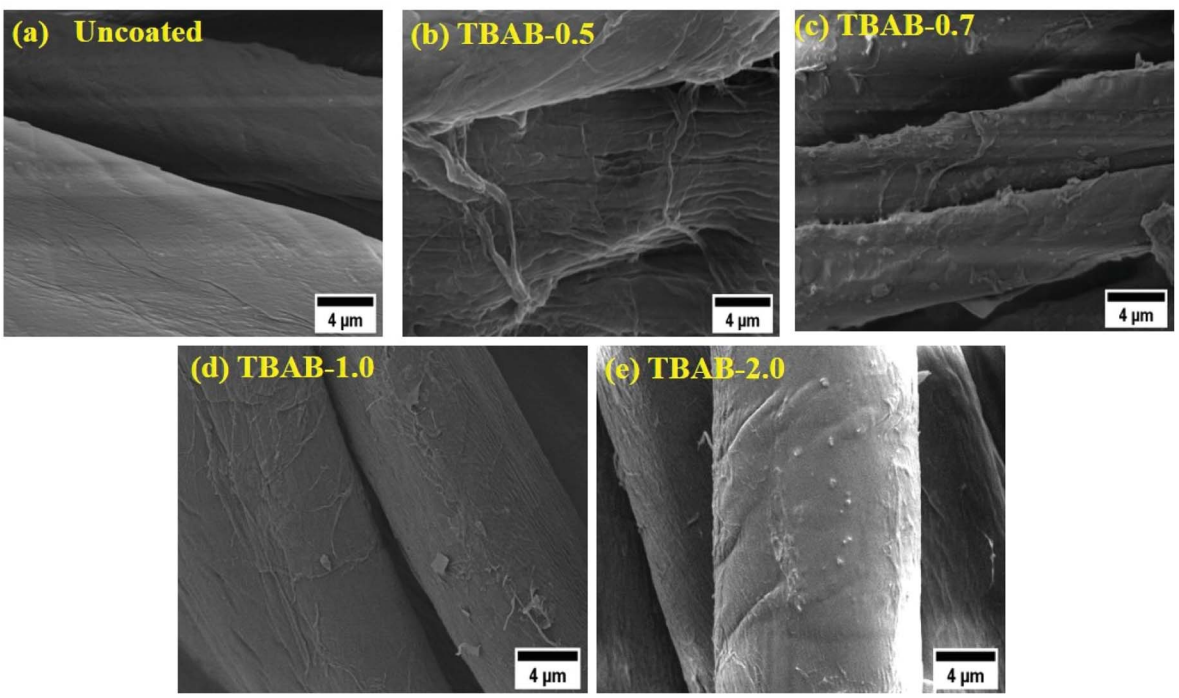

Fig. 4 (a–e) Detailed surface topographies of the uncoated and coated samples using LV-SEM.

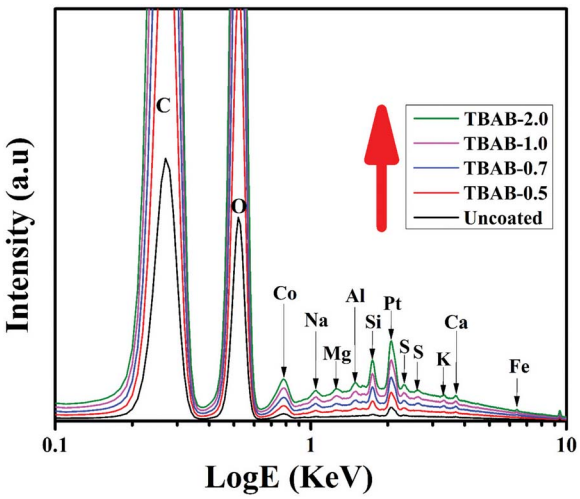

Fig. 5 EDX profile of the coated and uncoated samples.

Table 1 Elemental analysis of the coated and uncoated samples

Element	Uncoated	TBAB-0.5	TBAB-0.7	TBAB-1.0	TBAB-2.0
C	48.82	48.95	47.60	46.95	49.36
O	51.18	59.01	46.43	47.52	48.37
Na		0.70	1.15	0.06	0.64
Mg		**0.35**	**1.06**	**1.01**	**0.50**
Al		**1.09**	**2.10**	**2.08**	**0.91**
Si		**0.97**	**3.36**	**2.24**	**1.28**
S		0.13	0.09	0.04	0.10
Total	100	100	100	100	100

systems: Choi *et al.* obtained a range of 280–380 °C for 20BL whereas Carosio *et al.* obtained a range of 261–293 °C which is less protective than the current range.[28,34] However, this degradation trend is quite analogous to the results obtained for *ceramics* and even *intumescent* polymer layers.[28,50] Contrary to both of these studies, the current report could was not able to

Table 2 Thermogravimetric and derivative thermogravimetry data for uncoated and coated cotton

#	T_{onset}	T_{offset}	T_{peak1}	T_{peak2}	Total decomposition (%)
Uncoated	315.35	379.56	338.98	—	3.75
TBAB-0.5	310.32	383.40	356.41	368.03	8.32
TBAB-0.7	**329.92**	**394.48**	**335.26**	**365.50**	**17.02**
TBAB-1.0	316.86	370.43	342.71	360.51	12.86
TBAB-2.0	318.37	390.97	350.16	—	9.44

demonstrate a drop in the T_{onset} with the deposition of coatings due to the absence of the nitrogen or phosphorous-based species which could have caused earlier degradation. The obtained final residues are of high importance when considering the need to *calibrate* the fire-retardant behavior of samples. The residual mass can be ranked as: uncoated ~3.75% < TBAB 0.5–8.32% < TBAB 2.0–9.44 < TBAB 1.5–12.9 < TBAB ~0.7 to 17.0. The peak residue mass values were obtained for the TBAB 0.7–17.02, which is about 5 times more than that for the uncoated specimen. In comparison, the residue results were found superior by 2% and 6% than the values obtained by Pan *et al.* (500 °C and 700 °C respectively), using exfoliated layered double hydroxides and alginate.[51] Likewise Fang *et al.* used potassium alginate/polyhexamethylene guanidine phosphate solutions and obtained residue ~3.9% and 12.75% for 5BL and 20BL, which evidently suggest the significant superiority of this work (residue ~ 17.02%, 7BL).[52] This result could be attributed to the excellent protection by **TBAB-0.7** due its dense and MMT/VMT-rich coatings layers. Compared to the T_{onset}, which is quite higher for coated specimens, the peak degradation temperature of the **TBAB-0.7** was found as lowest ~335.26 °C; however, with a much lower degradation intensity, as can indicated in Fig. 6b. This could be possible due to the early peak degradation of the coatings contents to help form protective char. At T_{peak1} the major weight loss occurred due to the dehydration and decarboxylation by producing a maximum amount of volatiles gases

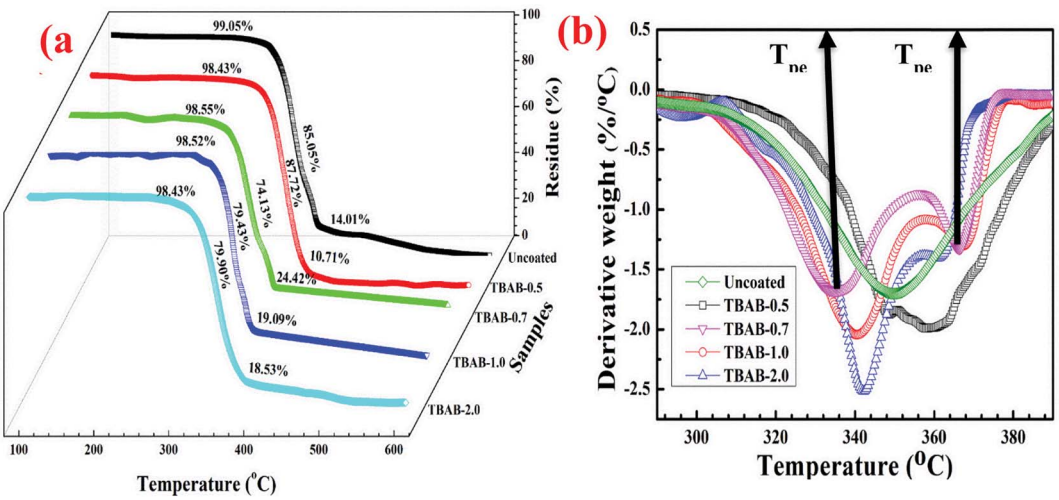

Fig. 6 (a, b) TGA and DTG curves of the coated and uncoated samples under nitrogen atmosphere.

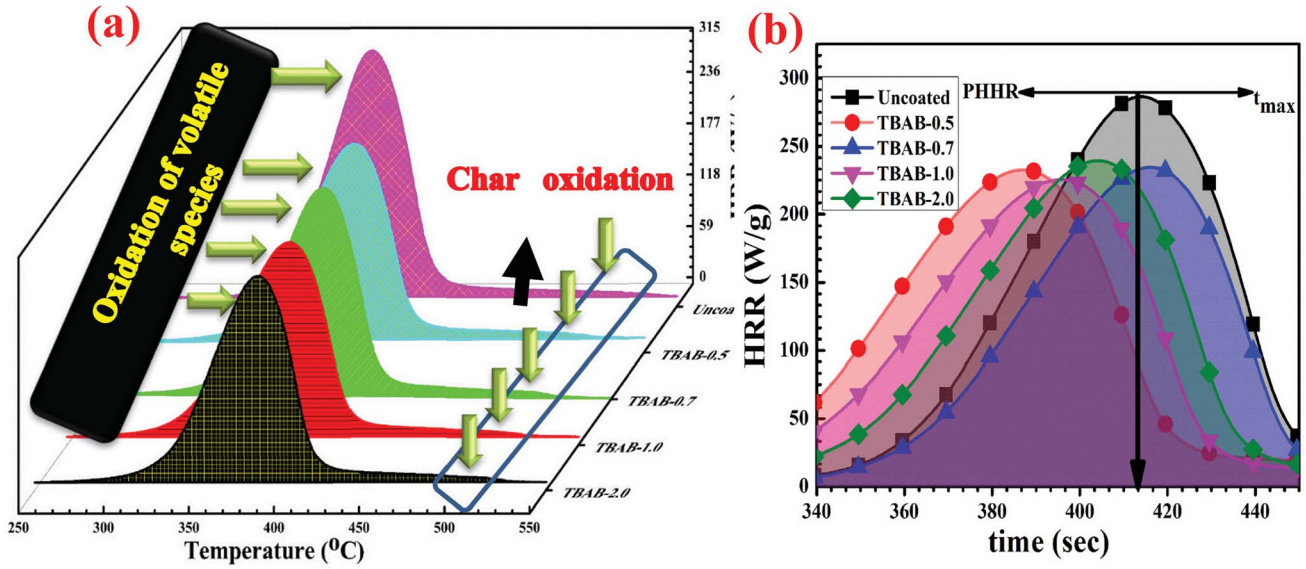

Fig. 7 Heat release curves obtained from MCC (a) HRR *vs.* "*T*" curves; (b) HRR *vs.* "*t*" (THR as area under the curves).

and char. The T_{peak2} is obtained due to the degradation of the char content and it has the highest value for **TBAB-0.7**, suggesting stable char, and hence, thermal stability which can be reflected from the residue values.

4.4 Pyrolysis–combustion analysis

Micro-combustion calorimetry (MCC) analysis of the coated and uncoated fabric was carried out to obtain the heat release curves as shown in Fig. 7a and b and to predict the thermal combustion properties. The time period, to stretch the peak of HRR for each test, increases as shown in Fig. 7b. The values of the peak of HRR steadily declines, however, until a maximum shift is obtained (for **TBAB-0.7**). The maximum thermal decomposition for all coatings studied herein occurred in a distinct temperature limit of 300–420 °C, which agrees with outcomes from TGA. The lowest peak HRR ~220.69 W g^{-1} for **TBAB-0.7**, compared to the 286.1 W g^{-1} for the uncoated samples, which accounts for a 23% reduction in the PHHR value. This reduction is highly comparable: the greater the value of HRR, the more transfer of the volatile species from the material surface. This notion would lead us to expect accelerating of the burning and pyrolysis. Therefore, the significant *decline* in the HRR values for **TBAB-0.7** indicates its effective role to protect the cotton fabric from degradation. It is important to note that the two step degradation phenomena and the char yield was obtained for both TGA and MCC tests which help signify the practicality of the results. Furthermore, need to mention that Carosio *et al.*, obtained mere 9% and 11% reduction in the PHRR and THR values for COT 400 specimens, compared to results achieved in his study as ~23% and ~30% reduction in the PHRR and THR values respectively. Though an expensive and synthetic branched polyethylene imine (BPEI) was used together with starch.[28]

The total heat release (THR) was derived from the time integral of the HRR profiles as shown in Fig. 7b. From the THR values, a remarkable decline can be observed for the coated samples, indicating lower heat content, and thus lower rates of combustion with a compared intensity to the uncoated samples. The THR reduced from 17.8 kJ g^{-1} for the uncoated fabric, to 12.5 kJ g^{-1} for **TBAB-0.7**, accounting for a ~30% decrease in the THR value of the sample as shown in Table 3. For instance, Fang *et al.*, achieved only 23% decrease in the THR values and that too for 20BL and using phosphate based LBL coatings.[52] It is believed that such reduction could have occurred in the major pyrolysis region (300–420 °C); this hints to the cause as being the inhibition of volatile gases by the coating layers. Likewise, the lowest THR value ~12.5, was found superior from the values

Table 3 Combustion and pyrolysis parameters obtained from MMC analysis

#	PHRR (W g^{-1}) reduction (%)	THR (kJ g^{-1}) reduction (%)	T_{PHHR} (°C)	T_{shou}	H_c (kJ g^{-1})	FIRGR (PHHR/t_{max})	m0	mf	Char yield (%)	HRC (J g^{-1} K^{-1})	LOI
Uncoated	286.61	17.79	371.73	—	18.73	0.771	13.9	0.7	5	408.35	21.795
TBAB-0.5	232.75 (−18)	17.23 (−3)	380.16	505.4	18.4	0.612	13.5	0.9	6.6	372.16	22.74
TBAB-0.7	**220.69 (−23)**	**12.45 (−30)**	**381.35**	**505.7**	**13.51**	**0.615**	**13.4**	**2.1**	**15.7**	**356.4**	**23.22**
TBAB-1.0	225.48 (−21)	15.28 (−14)	380.9	506.5	16.4	0.591	13.8	1	7.2	391.79	22.2
TBAB-2.0	239.61 (−16)	14.94 (−16)	381.5	512.6	15.73	0.628	13.9	0.7	5	390.58	22.24

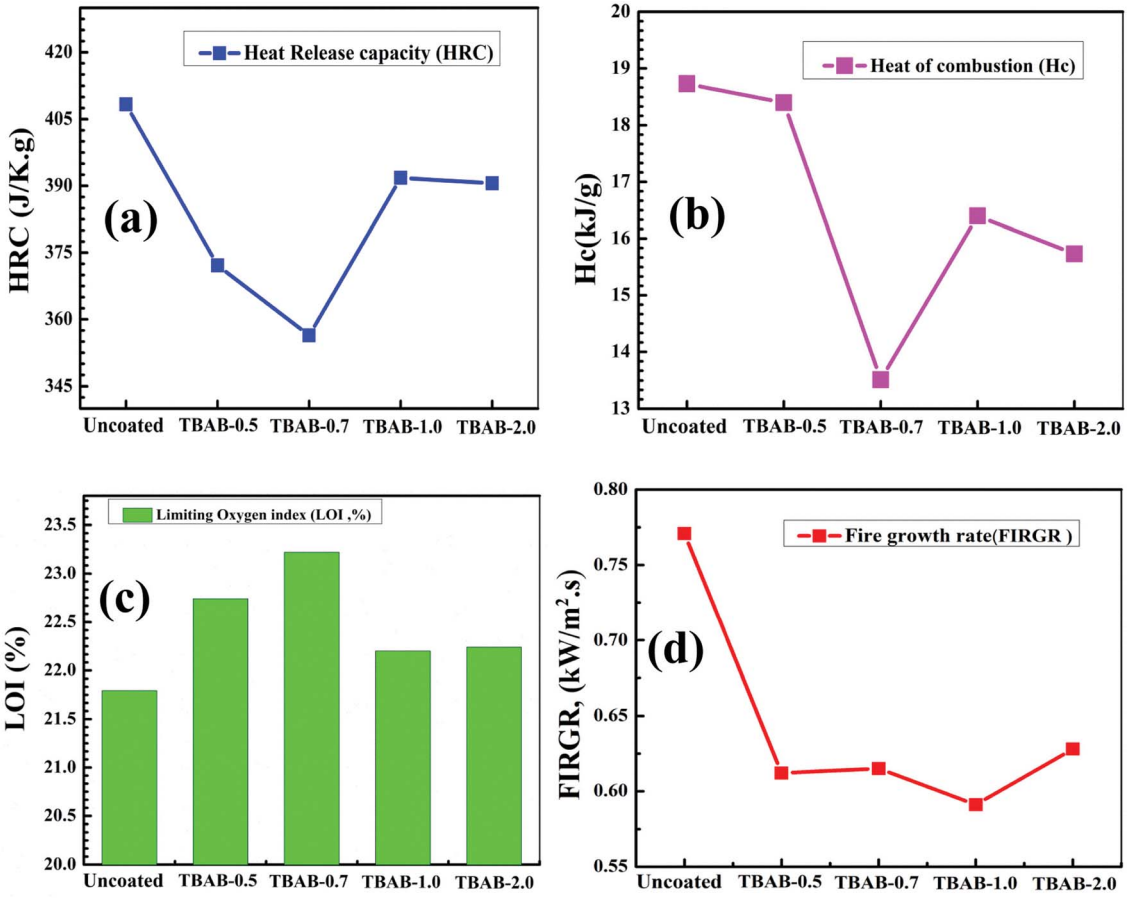

Fig. 8 Thermal parameters (a) HRC values for each coated sample; (b) H_c; (c) LOI; (d) FIRGR.

obtained by various authors as reported earlier.[53,54] Further, it is believed that THR and char yields have a strong *inverse* relationship. Thus, to achieve higher char yield, minimum heat release during combustion/pyrolysis process is required, which can be confirmed for the **TBAB-0.7** samples. The remarkable decrease in THR values for **TBAB-0.7** samples suggests enhanced inhibition and resistance against all the burning reactions (oxidative, pyrolysis, and combustion) mechanisms by the LBL layers. The possible reasons for the enhanced fire resistance by the coatings could include: optimized concentration of TBAB cationizing the agent to help produce highly charged starch and thus increase the intake of the clay species to the LBL matrix as a result of strong electrostatic attractions of the clay and the corresponding charged starch. On the contrary, more increasing the TBAB, it could be possible that the hydrolysis of starch is a step ahead of the cationization process which causes sluggish interaction forces during the LBL process or the larger weight of the starch molecule due to higher cationization values. The decrease in the interaction forces or heavy weight could result in the minimum intake of VMT/MMT particles and the formation of unwanted structural integration in the matrix, which could leave various *nano-zones* unshielded and easier to burn than those which remain shielded.

The median heat lost, as a result of the combustion of gram/degree, leads to a rise in temperature upon the pyrolysis interval which can be represented for heat release capacity (HRC) and plotted as shown in Fig. 8a. On the contrary to HRR and THR, the HRC is believed to be free of type, mass, and heating flow of the corresponding specimen and can be obtained through eqn (2) as reported previously.[53] The HRC values can be regarded as more reliable indicators relating to the materials capable of generating heat rise for each and every degree to the temperature during the combustion/pyrolysis. The heat release capacity can be observed and has been magnificently decline to ~356.4 J g^{-1} K^{-1} from ~408.4 J g^{-1} K^{-1} for the uncoated samples of **TBAB-0.7**; however, a further increase in the TBAB concentration could not cause any significant change in the HRC values. In contrast to HRR and THR, an immediate dramatic increase in values for HRC could be observed to higher values for uncoated **TBAB-1.0** and **TBAB-2.0** samples. This suggests that the heat content of the **TBAB-1.0** and **TBAB-2.0** could not significantly decrease with the coating, however, retarded by the coatings. A total of 12.7% reduction occurred for **TBAB-0.7**, in agreement with the result obtained for THR and HRR.

In addition to HRC, the sum of total heat of combustion (h_c) helps assess the total heat released by the material stack that transferred to gaseous substances plus char residue *via* the HRR experiment. The PHRR occurring temperature (T_{max}) and the residue are given in Table 3. The total heat of combustion (h_c) can be measured as reported.[55]

Fig. 9 (a–h) Vertical flame (UL-94) test of the samples; images after 15 s and final images of the residual char.

$$h_c = \frac{\mathrm{THR}}{1 - Y_p} \quad (1)$$

In eqn (1), THR (kJ g^{-1}) is the total heat release of the sample, whereas, the area under the resultant HRR curve, and "Y_p" represents the pyrolysis remaining (g g^{-1}). As shown in Fig. 8b, the total heat of combustion (pyrolyzed) portion plus the combustion zone of the sample (h_c) is decreased to a value of 13.5 kJ g^{-1} compared to 18.7 for the uncoated samples, accounting for 27.9% reduction. As observed, the THR reduction for **TBAB-0.7** was higher ~30%, which suggests that the difference could have been caused by the oxidation of the char residue.

Limiting oxygen index (LOI) values (Fig. 8c) were obtained for every coating derived herein.[55] An increase in the values of LOI can be observed for **TBAB-0.7**, however, with further increasing the cationizing agent, LOI values were found to decrease. More importantly, the decrease in the values of LOI could not occur as sharply as happened for the THR and h_c values. Thus, the decrease in the LOI values suggests no significant improvement in the combustion resistance of the coatings for highly cationized starch > 0.7 g. The Lyon equation of LOI can help anticipate the minimum oxygen concentration for flaming combustion and can be visualized for three separate contributions[56]

$$\mathrm{LOI} = \mathrm{OI} + \frac{\sigma T_{\mathrm{PHRR}}^4}{a} + \frac{\mathrm{HRR}^* \eta_g / aX^2}{(1-\mu)^2 \mathrm{HRC}} \quad (2)$$

(a) The least amount of oxygen required for the combustion of gaseous fuels relatively at a lower flammability limit. (b) Secondly is the ignition resistance ($\sigma T_{\mathrm{PHRR}}^4$) and the last but not least (c) is the resistance to burning (burning rate/pyrolysis). Therefore, the enhancement or the reduction in the LOI values could be linked to all these three fractions of the Lyon equation. It is stated that coatings with high LOI values has better defiance against the burning and ignition process in contrast to coatings with lower LOI. From Fig. 8c, it can be suggested that **TBAB-0.7** has the highest value and can be regarded as the best candidates of all coated samples. The values of LOI are considered as a "yardstick" for the ranking of flame-retardant characteristics of a material. A material is categorized as completely fire retardant if its LOI value > 26. In the current project, though it could not be achieved, however,

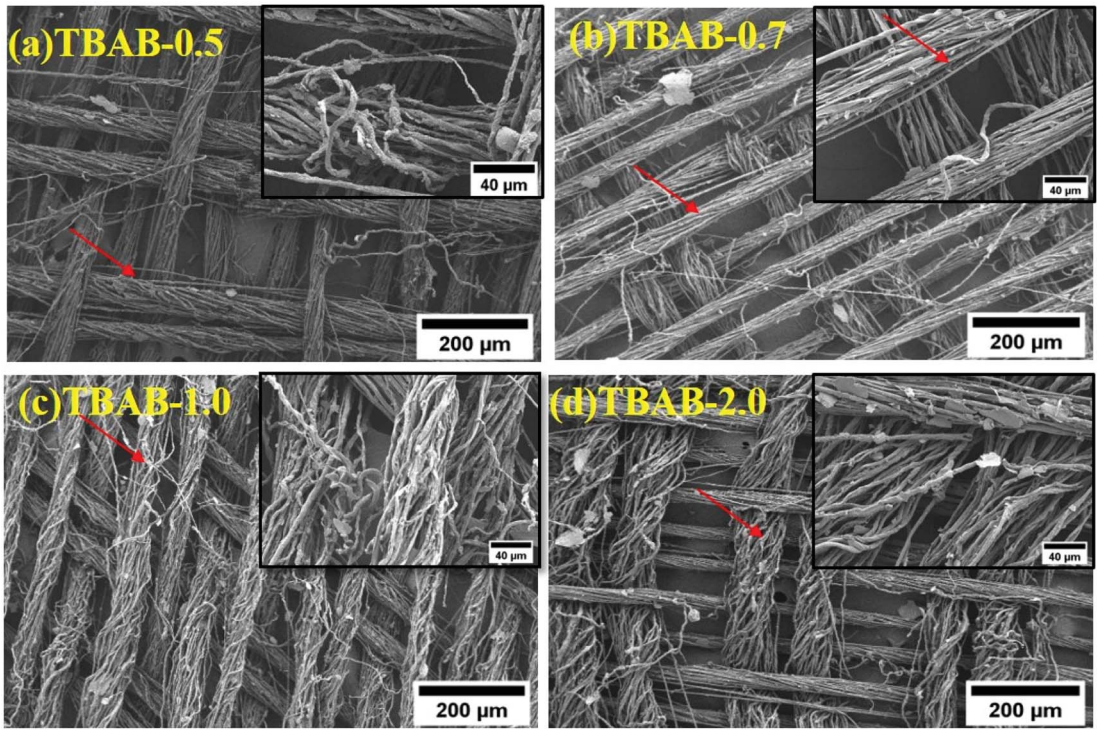

Fig. 10 (a–d) After-burn LV-SEM surface morphologies of char residue.

a significant increase in the LOI values can be observed in reference to the uncoated samples.

Finally, fire growth rates (FIGRA), which is PHHR divided by t_{PHHR} were plotted as shown in Fig. 8d. As the fire ignites, the growth stage can occur very fast, especially when the flame spread occurs; the neighboring heat feedback, fuel, and oxygen are easily available. Thus, it is believed that during the fire growth stage, the fire can be significantly controlled by obstructing the fuel source and hence protecting the fuel (sample) through the presence of the novel coating to help slow down the growth rate of the fire. The values of FIGRA is inversely proportional to the coating performance. As shown in Table 3, the lowest values among all other coated samples was observed for **TBAB-0.7**; hence, this is considered to be an excellent coating deposition.

To better investigate the flammability of the coated/uncoated fabric, vertical flame test trials (UL-94), (ASTM D6413) were conducted and the results can be seen in Fig. 9a–h. For the VFT test, a butane torch below the fabric sample was used for 10 s. The uncoated samples could not withstand the fire and burned rapidly by converting into ash within 2 s of the ignition. On contrary, the coated samples withstood the flame and converted to char instead of ash, which suggests that coating layers successfully suppressed the burning process. As shown in Fig. 9, after 15 s of ignition, for **TBAB-0.5**, the flame spread achieved the highest value compared to other coated samples. However, for **TBAB-0.7**, the flame spread reduced to a lowest value as shown in Fig. 9b. The reduced flame spread rate was possibly obtained as a consequence of physical barrier layers produced from effective polymer–clay–nanoparticle matrix (**TBAB-0.7**), as a result of effective cationization and thus improved adsorption. Increasing the TBAB content above 0.7 g L^{-1}, the rate of flame spread was further incremented for **TBAB-1.0** and **TBAB-2.0**, suggesting inferior resistance during the flame test. Furthermore, from the char images (Fig. 9e–h), it can be further seen that the uncoated samples disappeared after the burning process and no char was left behind (total loss/fire test). However, the samples (coated) exhibited significant formation of char lengths with highest value for **TBAB-0.7**, as can be seen in Fig. 9f. The fabric could have two possible reasons to break: (i) the intrinsic tensile stress and (ii) the external stress imparted by the holder. Due to the intrinsic stress the fabric could break at mid-points, while the external stress due to holder's attachment causes the breaking at the edges. The observations show that except **TBAB-0.7** rest of the samples (coated) were broken at their mid-point, which remained intact after the burning process, suggesting the effective structural integration role played by the coatings. Any flame retardant has a function of heat removing for the cellulosic fabrics, gas generation reduction, and combustion, to promote the char formation, prohibiting the access of oxygen to the flame, and tampering the oxidation of flammable substances. Subsequently, flame retardants (optimum) for cotton has the capacity of triggering the coating dehydration (water removal) process, hence functioning as a char prior to the condensed period as evidenced in the case of **TBAB-0.7**. It was explored, that there is a substantial decrease in the values of HRR/THR for the corresponding **TBAB-0.7** samples; nevertheless, the coatings may possibly not prevent the "blowout" of the vertical flame. This could be possible due to the lack of 100% correlation between the MCC

and UL-94 test for some parameters. The flame spread results are quite agreeable with the growth rate results calculated from the MCC data, which confirm the consistency in the experimental process and satisfactory correlation of the flammability and MCC tests.

4.5 After-burn surface analysis

Fig. 10a–d serves to explain the LV-SEM analysis of the char obtained from the vertical flame test; the inset images are zoomed in close ups of areas of interest. The difference between the samples can be clearly observed from the structural aberrations to the char fibers, broken portions and the presence of debris. It can be seen that the structure of every mesh shrunk by the burning process; the fire debris can be seen inside the single mesh as indicated by the arrows. However, such shrinkage of the mesh structure cannot be observed in the **TBAB-0.7**, suggesting the flame faces obstruction to access deep inside the mesh of the experimental material. In addition, the mesh symmetry was significantly damaged by the burning process; this might be due to the plastic deformation. Thus, the empty zones between the meshes have been highly misplaced caused by the burning process. However, there cannot be seen any broken part or change of mesh symmetry in the case of **TBAB-0.7** upon burning, suggesting significant mechanical stability of the sample against the burning process. In addition, the surface layers of **TBAB-0.7** can be seen as dense and compact, thought to serve to obstruct the passage and currents of hot gases. This in turn helps reduce the production of the commonly formed gases including CO and CO_2. The observed HRR which is low for **TBAB-0.7** and the observed degradation temperature differed from those of untreated materials and require some tentative explanation as such. The deposition of the char produced, therefore, is a result of a pyrolysis mechanism of this cationized starch material; char will affect the volume/concentration of combustible gas produced. Comparing the inset plot in Fig. 10b and the obtained surface morphologies by,[28] the broken portions and structural aberrations occurred in this study are quite less significant, suggesting the enhanced structural integrations of the current coated samples.

5. Conclusion

TBAB–based cationized starch was used to produce novel materials that are cotton coated with nanomaterials layers that help achieve flame retardancy. LV-SEM analysis explored, that cotton fibers up to the singular level were coated uniformly by the dense coating layers, particularly the **TBAB-0.7**. Two modes of deposition phenomena appeared active: precipitate-type and uniform-type, further confirmed by EDX analysis. The peak range of the degradation was highly improved from lower range to higher range (329.9–394.5 °C), together with significant mass residue for TBAB-0.7–17.0% as measured through TGA analysis. A significant reduction in the thermal parameters (PHRR $\sim$ 23%, THR $\sim$ 30%, $H_c \sim 27.9\%$) was obtained, for **TBAB-0.7**, suggesting the enhanced fire resistance role of the sample and in agreement to the TGA results. The LOI values were witnessed increase with cationizing agent, to a maximum value for **TBAB-0.7**. The VFT test and after burn analysis revealed a lack of char for the uncoated sample; however, a maximum char with enhanced mechanical stability and integrity was achieved for **TBAB-0.7**.

Conflicts of interest

There are no conflicts to declare.

Acknowledgements

The work is supported by the Ministry of Education (Korea National Research Foundation, 2018R1A6A1A03024509 and 2021R1I1A1A01055102), KAIST, and Molecular Logic Gate Laboratory, D. G. C. the KAIX Program (KAIST).

Notes and references

1 P. Wakelyn and G. Gamble, *Cotton fiber chemistry and technology*, 2007, pp. 23–68.
2 F. Yang, Z. Cai, P. Wang and X. Yang, *J. Nanotechnol. Mater. Sci.*, 2017, **4**, 48–52.
3 P. Reddy, G. Agathian and A. Kumar, *Radiat. Phys. Chem.*, 2005, **72**, 511–516.
4 H. Yuan, W. Xing, P. Zhang, L. Song and Y. Hu, *Ind. Eng. Chem. Res.*, 2012, **51**, 5394–5401.
5 K. Xie, A. Gao and Y. Zhang, *Carbohydr. Polym.*, 2013, **98**, 706–710.
6 J. Alongi and G. Malucelli, *J. Mater. Chem.*, 2012, **22**, 21805–21809.
7 J. Alongi, F. Carosio and G. Malucelli, *Polym. Degrad. Stab.*, 2014, **106**, 138–149.
8 K. M. Holder, R. J. Smith and J. C. Grunlan, *J. Mater. Sci.*, 2017, **52**, 12923–12959.
9 Z. Ur Rehman, H. Seok-Hwan, U. Zakir, P. Ye-Tang, D. G. Churchill and B. H. Koo, *Carbohydr. Polym.*, 2021, **274**, 118626–118637.
10 S. T. Lazar, T. J. Kolibaba and J. C. Grunlan, *Nat. Rev. Mater.*, 2020, **5**, 259–275.
11 A.-L. Davesne, M. Jimenez, F. Samyn and S. Bourbigot, *Prog. Org. Coat.*, 2021, **154**, 106217.
12 O. Köklükaya, R.-M. P. Karlsson, F. Carosio and L. Wågberg, *Carbohydr. Polym.*, 2021, **255**, 117468.
13 G. Decher, *Multilayer Thin Films*, 2003, 1–46.
14 P. Bertrand, A. Jonas, A. Laschewsky and R. Legras, *Macromol. Rapid Commun.*, 2000, **21**, 319–348.
15 G. Fleer, M. C. Stuart, J. M. Scheutjens, T. Cosgrove and B. Vincent, *Polymers at interfaces*, Springer Science & Business Media, 1993.
16 K. Ariga, Y. M. Lvov and G. Decher, *Phys. Chem. Chem. Phys.*, 2021, DOI: 10.1039/D1CP04669A.
17 F. Lv, Z. Peng, L. Zhang, L. Yao, Y. Liu and L. Xuan, *Liq. Cryst.*, 2009, **36**, 43–51.
18 Y. Shimazaki, R. Nakamura, S. Ito and M. Yamamoto, *Langmuir*, 2001, **17**, 953–956.

19 J. Sun, T. Wu, F. Liu, Z. Wang, X. Zhang and J. Shen, *Langmuir*, 2000, **16**, 4620–4624.
20 O. Mermut and C. J. Barrett, *J. Phys. Chem. B*, 2003, **107**, 2525–2530.
21 Z. Sui, D. Salloum and J. B. Schlenoff, *Langmuir*, 2003, **19**, 2491–2495.
22 R. A. McAloney, M. Sinyor, V. Dudnik and M. C. Goh, *Langmuir*, 2001, **17**, 6655–6663.
23 L. Chang, X. Kong, F. Wang, L. Wang and J. Shen, *Thin Solid Films*, 2008, **516**, 2125–2129.
24 Y. Pan, J. Zhan, H. Pan, W. Wang, G. Tang, L. Song and Y. Hu, *ACS Sustainable Chem. Eng.*, 2016, **4**, 1431–1438.
25 G. Tondi, W. Zhao, A. Pizzi, G. Du, V. Fierro and A. Celzard, *Bioresour. Technol.*, 2009, **100**, 5162–5169.
26 T.-T. Yang, J.-P. Guan, R.-C. Tang and G. Chen, *Ind. Crops Prod.*, 2018, **115**, 16–25.
27 J. Alongi, R. A. Carletto, A. Di Blasio, F. Carosio, F. Bosco and G. Malucelli, *J. Mater. Chem. A*, 2013, **1**, 4779–4785.
28 F. Carosio, G. Fontaine, J. Alongi and S. Bourbigot, *ACS Appl. Mater. Interfaces*, 2015, **7**, 12158–12167.
29 L. Costes, F. Laoutid, S. Brohez and P. Dubois, *Mater. Sci. Eng., R*, 2017, **117**, 1–25.
30 K. Wu, Y. Hu, L. Song, H. Lu and Z. Wang, *Ind. Eng. Chem. Res.*, 2009, **48**, 3150–3157.
31 I. Tsuyumoto, Y. Miura, M. Nirei, S. Ikurumi and T. Kumagai, *J. Mater. Sci.*, 2011, **46**, 5371–5377.
32 R. Davis, Y.-C. Li, M. Gervasio, J. Luu and Y. S. Kim, *ACS Appl. Mater. Interfaces*, 2015, **7**, 6082–6092.
33 B. N. Mallick, P. K. Rana and P. K. Sahoo, *Adv. Polym. Technol.*, 2015, **34**, 21519–21526.
34 K. Choi, S. Seo, H. Kwon, D. Kim and Y. T. Park, *J. Mater. Sci.*, 2018, **53**, 11433–11443.
35 A. A. Owodunni, R. Hashim, O. F. A. Taiwo, M. H. Hussin, M. H. M. Kassim, Y. Bustami, O. Sulaiman, M. H. M. Amini and S. Hiziroglu, *J. Phys. Sci.*, 2020, **31**, 129–143.
36 S. Suvorov and V. Skurikhin, *Refract. Ind. Ceram.*, 2003, **44**, 186–193.
37 J. Addison, *Regul. Toxicol. Pharmacol.*, 1995, **21**, 397–405.
38 A. Cain, M. Plummer, S. Murray, L. Bolling, O. Regev and J. C. Grunlan, *J. Mater. Chem. A*, 2014, **2**, 17609–17617.
39 S. Ortelli, G. Malucelli, F. Cuttica, M. Blosi, I. Zanoni and A. L. Costa, *Cellulose*, 2018, **25**, 2755–2765.
40 S. Ortelli, G. Malucelli, M. Blosi, I. Zanoni and A. L. Costa, *J. Colloid Interface Sci.*, 2019, **546**, 174–183.
41 K. Apaydin, A. Laachachi, V. Ball, M. Jimenez, S. Bourbigot and D. Ruch, *Colloids Surf., A*, 2015, **469**, 1–10.
42 S. Qin, M. G. Pour, S. Lazar, O. Köklükaya, J. Gerringer, Y. Song, L. Wågberg and J. C. Grunlan, *Adv. Mater. Interfaces*, 2019, **6**, 1801424.
43 Z. U. Rehman, A. K. Niaz, J.-I. Song and B. H. Koo, *Polymers*, 2021, **13**, 303.
44 M. Kweon, P. Bhirud and F. S. Saskatoon, *Starch/Staerke*, 1996, **48**, 214–220.
45 M. Hasani, E. D. Cranston, G. Westman and D. G. Gray, *Soft Matter*, 2008, **4**, 2238–2244.
46 L. Yan, H. Tao and P. R. Bangal, *Clean: Soil, Air, Water*, 2009, **37**, 39–44.
47 M. Zaman, H. Xiao, F. Chibante and Y. Ni, *Carbohydr. Polym.*, 2012, **89**, 163–170.
48 M. Shirazi, T. G. van de Ven and G. Garnier, *Langmuir*, 2003, **19**, 10829–10834.
49 J. W. Ostrander, A. A. Mamedov and N. A. Kotov, *J. Am. Chem. Soc.*, 2001, **123**, 1101–1110.
50 J. C. Yang, W. Liao, S. B. Deng, Z. J. Cao and Y. Z. Wang, *Carbohydr. Polym.*, 2016, **151**, 434–440.
51 H. Pan, W. Wang and Q. Shen, *RSC Adv.*, 2016, **6**, 111950–111958.
52 F. Fang, X. Chen, X. Zhang, C. Cheng, D. Xiao, Y. Meng, X. Ding, H. Zhang and X. Tian, *Prog. Org. Coat.*, 2016, **90**, 258–266.
53 C. Q. Yang, Q. He, R. E. Lyon and Y. Hu, *Polym. Degrad. Stab.*, 2010, **95**, 108–115.
54 R. Lyon, R. Walters, S. Stoliarov, N. Safronava, *Principles and Practice of Microscale Combustion Calorimetry*, Federal Aviation Administration, 2013.
55 Q. Xu, C. Jin, A. Majlingova and A. Restas, *J. Therm. Anal. Calorim.*, 2018, **133**, 649–657.
56 F. Carosio, C. Negrell-Guirao, A. Di Blasio, J. Alongi, G. David and G. Camino, *Carbohydr. Polym.*, 2015, **115**, 752–759.